

Spectroscopy of the neutron-deficient nucleus $^{167}\text{Os}_{91}$

D. O'Donnell,^{1,*} T. Grahn,² D. T. Joss,² J. Simpson,¹ C. Scholey,³ K. Andgren,⁴ L. Bianco,² B. Cederwall,⁴ D. M. Cullen,⁵ A. Dewald,⁶ E. Ganioglu,^{4,7} M. B. Gómez Hornillos,^{1,†} P. T. Greenlees,³ B. Hadinia,^{4,‡} H. Iwasaki,⁶ U. Jakobsson,³ J. Jolie,⁶ P. Jones,³ D. S. Judson,² R. Julin,³ S. Juutinen,³ S. Ketelhut,³ M. Labiche,¹ M. Leino,³ N. M. Lumley,⁵ P. J. R. Mason,⁵ O. Möller,⁸ P. Nieminen,³ M. Nyman,³ R. D. Page,² J. Pakarinen,^{3,§} E. S. Paul,² M. Petri,^{2,||} A. Petts,² P. Peura,³ N. Pietralla,⁸ Th. Pissulla,⁶ P. Rahkila,³ P. Ruotsalainen,³ M. Sandzelius,^{3,4} P. J. Sapple,² J. Sarén,³ J. Sorri,³ J. Thomson,² J. Uusitalo,³ and H. V. Watkins²

¹STFC, Daresbury Laboratory, Daresbury, Warrington WA4 4AD, United Kingdom

²Oliver Lodge Laboratory, University of Liverpool, Liverpool L69 7ZE, United Kingdom

³Department of Physics, University of Jyväskylä, P. O. Box 35, FI-40014 Jyväskylä, Finland

⁴Department of Physics, Royal Institute of Technology, Alba Nova Centre, SE-10691 Stockholm, Sweden

⁵Department of Physics and Astronomy, University of Manchester, Manchester M13 9PL, United Kingdom

⁶Institut für Kernphysik, Universität zu Köln, D-50937 Köln, Germany

⁷Science Faculty, Physics Department, Istanbul University, TR-34459 Istanbul, Turkey

⁸Institut für Kernphysik, TU Darmstadt, D-64289 Darmstadt, Germany

(Received 24 February 2009; published 10 June 2009)

Excited states of the nucleus ^{167}Os have been populated by the reaction $^{92}\text{Mo}(^{78}\text{Kr}, 2pn)$. The JUROGAM γ -ray detector array has been used in conjunction with the RITU gas-filled separator and the GREAT spectrometer to observe prompt γ rays in coincidence with recoiling fusion-evaporation residues and their subsequent decay by α particle emission. By correlating prompt γ radiation with the characteristic α radioactivity of ^{167}Os , it has been possible to extend the level scheme for this nucleus significantly. In particular, an extension of the yrast band and four previously unobserved bands are reported. In addition, the recoil distance Doppler-shift method was used to determine a lifetime of $\tau = 20(4)$ ps for the $I^\pi = 17/2^+$ state in ^{167}Os . Hence, the level of collectivity and magnitude of deformation of the low spin yrast band of this nucleus is established.

DOI: [10.1103/PhysRevC.79.064309](https://doi.org/10.1103/PhysRevC.79.064309)

PACS number(s): 23.20.Lv, 21.10.Tg, 25.70.Gh, 27.70.+q

I. INTRODUCTION

Recent experiments employing selective tagging techniques [1–3] have established excited states in the neutron-deficient osmium isotopes [4–8] down to ^{162}Os and have revealed changes in the underlying nuclear structure as the closed shell at $N = 82$ is approached. A gradual evolution in the structure of Os isotopes is evident when moving from the neutron midshell at $N = 104$, where the nuclei display behavior typical of stable prolate deformations, through to shape coexistence in ^{172}Os ($N = 96$) [9], and toward sphericity in ^{162}Os [4]. This behavior is clearly demonstrated in the ratio of the energies of the first excited $I^\pi = 2^+$ and 4^+ states, $E(4^+)/E(2^+)$. At the neutron midshell, even- A Os nuclei have an excitation energy ratio $E(4^+)/E(2^+)$ close to the limit of an ideal rotating nucleus (3.3). This ratio is observed to decrease as a function of N for $N < 104$ and by ^{164}Os the ratio reaches the value of 2.4 [5], close to the ideal value of 2.5 for a γ -soft rotor.

The spectroscopy of odd- A nuclei is particularly important in identifying the active single-particle orbitals and their core-polarizing influence. In this work, excited states based on several single-neutron states have been established to high spin in ^{167}Os . In addition, lifetime information is particularly rare in these extremely neutron-deficient nuclei. In the case of Os nuclei the lightest nucleus in which lifetime information has been reported is ^{172}Os [10]. The lifetime of the $17/2^+$ state in the yrast band of ^{167}Os has been measured in this work providing information on the extent of nuclear deformation.

The nucleus ^{167}Os represents the lightest odd- A isotope of Os in which detailed spectroscopy has thus far been possible [7]. However, the level scheme reported in the work of Joss *et al.* [7] was constructed from a γ - γ analysis with events correlated solely with the detection of a recoiling fusion-evaporation residue at the focal plane of the RITU separator. In the present study, it has been possible to correlate the γ - γ data with the characteristic α decays of ^{167}Os .

In a recent study of isomeric states in this region, Scholey *et al.* [11], using one of the same data sets as discussed in the present work, have identified the decay path to the $I^\pi = 7/2^-$ ground state from the $13/2^+$ state in ^{167}Os [11]. This state decays via a 348-keV γ ray with a half-life of 672(7) ns [11]. The 348-keV transition was reported to feed the first excited state of ^{167}Os at 87 keV. The band feeding this state promptly is reported here for the first time. In addition, the present work has revealed another band, also observed to bypass the $I^\pi = 13/2^+$ isomer, which is thought to decay directly to the ^{167}Os ground state.

* david.o'donnell@stfc.ac.uk

[†]Present address: Department of Physics and Nuclear Engineering, Universitat Politècnica de Catalunya, Barcelona, Spain.

[‡]Present address: School of Engineering and Science, University of the West of Scotland, Paisley PA1 2BE, United Kingdom.

[§]Present address: Oliver Lodge Laboratory, University of Liverpool, Liverpool L69 7ZE, United Kingdom.

^{||}Present address: Nuclear Science Division, Lawrence Berkeley National Laboratory, Berkeley, California 94720, USA.

The yrast sequence of ^{167}Os [7], which is based on the $13/2^+$ state, has been extended with the observation of three new excited states. This has allowed the properties and characteristics of this band to be studied in more detail than was previously possible. Furthermore, additional non-yrast bands that decay to the yrast band are also reported for the first time.

II. EXPERIMENTAL DETAILS AND ANALYSIS

A. Recoil decay tagging experiments

The excited states of ^{167}Os were populated via the $2pn$ evaporation channel following the fusion of a ^{78}Kr beam with a ^{92}Mo target of thickness $550 \mu\text{g}/\text{cm}^2$. The observations reported here are the results of three separate experiments in which the beam was accelerated to an energy of 335 MeV for ~ 162 h, 357 MeV for ~ 23 h, and 365 MeV for ~ 65 h. On all three occasions, the $^{78}\text{Kr}^{15+}$ beam was provided at intensities of 5–8 pA by the K130 cyclotron of the Accelerator Laboratory of the University of Jyväskylä. At the target position, the JUROGAM Ge-detector array [12] was used to detect the prompt γ rays emitted by the recoiling fusion-evaporation residues. The gas-filled separator RITU [13] was used to transport the reaction products to the focal plane where they were detected using the GREAT spectrometer [14]. α - and γ -ray spectroscopy of the recoils was facilitated by two adjacent double-sided silicon strip detectors (DSSDs), a planar Ge detector, a high-efficiency clover Ge detector, and an array of 28 Si PIN diode detectors. A multiwire proportional counter provided energy loss and (in conjunction with the DSSDs) time-of-flight information, which allowed the recoils to be distinguished from the scattered beam.

The characteristic α decays of ^{167}Os $\{E_\alpha = 5853(5) \text{ keV}, T_{1/2} = 0.84(7) \text{ s}$ [15] $\}$ are labeled in Fig. 1(a) that shows all α particles observed in the DSSDs at the focal plane within 2.15 seconds [$\sim 2.5 \times T_{1/2}(^{167}\text{Os})$] of the detection of a recoil. The cross section for the population of ^{167}Os via the $2pn$ channel is estimated to be $\sim 0.6 \text{ mb}$. The ^{167}Os α decays were temporally correlated with γ rays detected at the target position [see Fig. 1(b)]. A number of γ -ray transitions that have been identified as originating in ^{168}Os ($T_{1/2} = 2.1(1) \text{ s}$ [15]) can also be seen in Fig. 1(b). This is an unfortunate consequence of the relatively long correlation time used in the current analysis. In the analysis the average recoil implantation rate in the DSSDs was $\approx 450 \text{ Hz}$. These data were sorted using the Grain program [16] and the γ - γ analysis was performed using the RADWARE software suite [17].

B. RDDS lifetime measurement

For the recoil distance Doppler-shift (RDDS) lifetime measurement of ^{167}Os , the $^{92}\text{Mo}(^{78}\text{Kr}, 2pn)^{167}\text{Os}$ reaction at a beam energy of 336 MeV was used. With a stretched $1\text{-mg}/\text{cm}^2$ ^{92}Mo target, this reaction provided an initial recoil velocity of $v/c = 3.8\%$. The Köln plunger device, housing both the ^{92}Mo target and a Mg degrader foil of thickness $1 \text{ mg}/\text{cm}^2$, was installed at the JUROGAM target position. The replacement of a standard stopper foil of the plunger device by the degrader foil allowed the evaporation residues to recoil into RITU. Prompt singles γ -ray spectra tagged with the ^{167}Os α

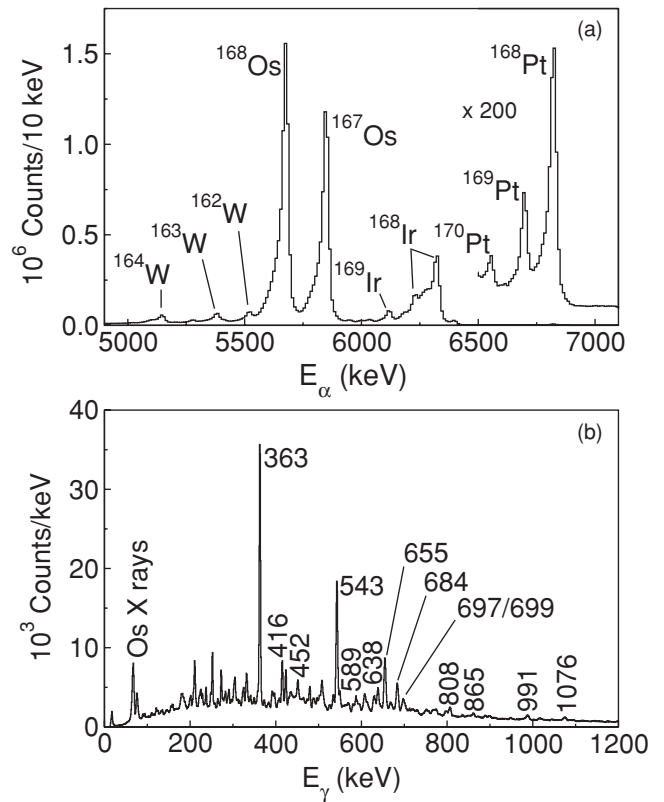


FIG. 1. (a) All α particles observed in the DSSDs within 2.15 s of the implantation of a recoil. The presence of ^{170}Pt , in addition to the intensity of the ^{169}Pt peak, is attributed to target impurities. (b) γ rays observed in tagging on the characteristic α decay of ^{167}Os . This spectrum was obtained from the 365-MeV reaction. Some of the peaks that are unmarked have been identified as resulting from other reaction channels.

decays, as described in Sec. II A, were recorded at 13 different target to degrader distances, ranging from $5 \mu\text{m}$ to 8 mm.

It should be noted that this experiment was optimized for the study of ^{168}Os . Hence, due to limited statistics, a lifetime could only be measured reliably for the $I^\pi = 17/2^+$ state in ^{167}Os . Decay curves $I_d/(I_s + I_d)$, where I_s and I_d are intensities of fully Doppler-shifted and degraded components, respectively, were extracted from the γ -ray spectra recorded with five Ge detectors with $\theta = 158^\circ$ and 10 with $\theta = 134^\circ$, with respect to the beam direction. Typical separation of the fully Doppler-shifted and degraded components in the γ -ray spectra was of the order of 4 keV at $\sim 450 \text{ keV}$ at 134° . The decay curves were analyzed using the differential decay curve method (DDCM) [18]. Examples of typical spectra are illustrated in Fig. 2.

III. EXPERIMENTAL RESULTS

A. Extension of ^{167}Os level scheme

The level scheme of ^{167}Os , shown in Fig. 3, was constructed on the basis of observed γ -ray intensities and γ - γ coincidences. The properties of the γ -ray transitions can be found in Table I. The multipolarity of a number of the transitions has been estimated by means of angular correlations. In the present

TABLE I. Properties of γ rays associated with the decay of ^{167}Os as a result of the present work. Intensities I_γ are normalized to the 363-keV transition, $17/2^+ \rightarrow 13/2^+$. Angular intensity ratios R have been measured by demanding coincidences with 363-keV transition unless specified otherwise. Representative values, measured here, for a proposed stretched $E1$ transition and a proposed stretched $E2$ transition in ^{168}Os [7] are also listed for comparison. These values were in coincidence with the 341-keV $2^+ \rightarrow 0^+$ transition. Spin and parity assignments are listed.

E_γ (keV)	I_γ (%)	R	$I_{\text{initial}}^\pi \rightarrow I_{\text{final}}^\pi$
87.1 ± 0.1	1.7 ± 0.1		$9/2^- \rightarrow 7/2^-$
210.5 ± 0.4	3.3 ± 0.1		
303.6 ± 0.2	3.9 ± 0.4		$(27/2^-) \rightarrow (23/2^-)$
362.9 ± 0.1	100 ± 0.1	1.28 ± 0.06^a	$17/2^+ \rightarrow 13/2^+$
415.8 ± 0.2	32.9 ± 0.4	0.92 ± 0.18^b	$13/2^- \rightarrow 9/2^-$
451.5 ± 0.1	13.8 ± 0.3	0.93 ± 0.18^c	$11/2^- \rightarrow 7/2^-$
479.6 ± 0.1	4.0 ± 0.4		$(27/2^-) \rightarrow (23/2^-)$
488.4 ± 0.4	0.3 ± 0.1		
497.6 ± 0.1	1.8 ± 0.1		$(31/2^-) \rightarrow (27/2^-)$
513.9 ± 0.2	2.0 ± 0.5		$(27/2^-) \rightarrow 25/2^+$
534.3 ± 0.4	2.1 ± 0.5		$(31/2^-) \rightarrow (27/2^-)$
543.2 ± 0.1	65.5 ± 0.6	1.37 ± 0.07	$21/2^+ \rightarrow 17/2^+$
588.5 ± 0.1	16.7 ± 0.3	0.81 ± 0.16^d	$(17/2^-) \rightarrow 13/2^-$
609.3 ± 0.1	9.8 ± 0.2	1.18 ± 0.26^e	$15/2^- \rightarrow 11/2^-$
632.5 ± 0.1	3.9 ± 0.5		$(27/2^-) \rightarrow 25/2^+$
637.9 ± 0.3	2.4 ± 0.5		$(33/2^+) \rightarrow 29/2^+$
644.9 ± 0.2	3.6 ± 1.0		
655.3 ± 0.1	32.2 ± 0.4	1.47 ± 0.13	$25/2^+ \rightarrow 21/2^+$
666.2 ± 0.4	0.8 ± 0.3		$(37/2^+) \rightarrow (33/2^+)$
672.3 ± 0.2	1.0 ± 1		$(35/2^-) \rightarrow (31/2^-)$
684.1 ± 0.1	11.2 ± 0.2	1.54 ± 0.26	$29/2^+ \rightarrow 25/2^+$
697.4 ± 0.1	2.6 ± 2.2		$(19/2^-) \rightarrow (15/2^-)$
698.5 ± 0.1	7.6 ± 1.5	0.83 ± 0.25^d	$(21/2^-) \rightarrow (17/2^-)$
750.4 ± 0.3	2.9 ± 0.6		
766.9 ± 0.4	3.3 ± 0.5		$(25/2^-) \rightarrow (21/2^-)$
807.5 ± 0.1	5.3 ± 0.2	0.54 ± 0.32	$(23/2^-) \rightarrow 21/2^+$
865.4 ± 0.2	4.8 ± 0.5	0.24 ± 0.39	$(23/2^-) \rightarrow 21/2^+$
901.3 ± 0.4	0.2 ± 1.1		
990.8 ± 0.1	3.9 ± 0.2		
1076.4 ± 0.6	9.8 ± 0.4		
^{168}Os : 880	$E1$ [7]	0.85 ± 0.06	$(5^-) \rightarrow 4^+$
^{168}Os : 642	$E2$ [7]	1.18 ± 0.05	$6^+ \rightarrow 4^+$

^aMeasured in coincidence with 543-keV transition.

^bMeasured in coincidence with 589-keV transition.

^cMeasured in coincidence with 609-keV transition.

^dMeasured in coincidence with 416-keV transition.

^eMeasured in coincidence with 452-keV transition.

work, angular-intensity ratios have been calculated using the relation,

$$R = \frac{I_\gamma(158^\circ)}{I_\gamma(108^\circ + 72^\circ)},$$

where $I_\gamma(\theta)$ represents the efficiency-corrected intensity of the γ ray in detectors located at an angle θ subject to the condition that a coincident γ ray was observed at any angle. For each ratio, the gating transition is given in the footnote of Table I. Measured values for a proposed stretched $E1$ transition and a

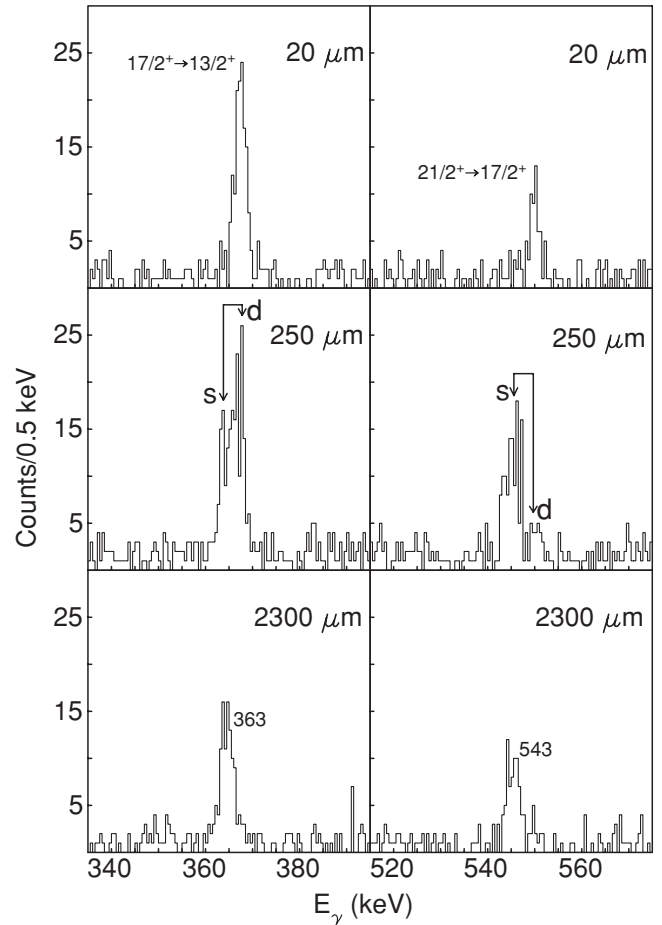


FIG. 2. Typical ^{167}Os α -selected γ -ray singles spectra recorded by the 10 JUROGAM detectors at 134° at three different target to degrader distances. The position of the fully Doppler-shifted (s) and degraded (d) components of the γ -ray transitions is indicated for the intermediate distance.

proposed stretched $E2$ transition [7] in ^{168}Os are also included in Table I to provide a reference.

Excited states of ^{167}Os were first observed by Joss *et al.* [7], who reported three band structures and a total of nine transitions. The yrast band was attributed to a rotational sequence built on a neutron $i_{13/2}$ intruder configuration, consistent with expectations based on the heavier Os isotopes [8,19–21]. The other two bands are designated as Bands 4 and 5 in Fig. 3. Typical γ -ray coincidence spectra, correlated with the α decay of ^{167}Os , are shown in Figs. 4 and 5.

Figure 4(a) shows the energy spectrum of γ rays observed in coincidence with the 543-keV transition, which confirms the yrast band transitions reported by Joss *et al.* [7]. In addition, two transitions of energies 638 and 666 keV have been observed, extending the yrast band to higher spin; see Figs. 4(b) and 4(c). Of the transitions that have been associated with the decay of the yrast band in the present study, it has been possible to infer the multipolarity of all but two through angular-intensity ratio measurements. This analysis suggest the transitions display behavior consistent with quadrupole

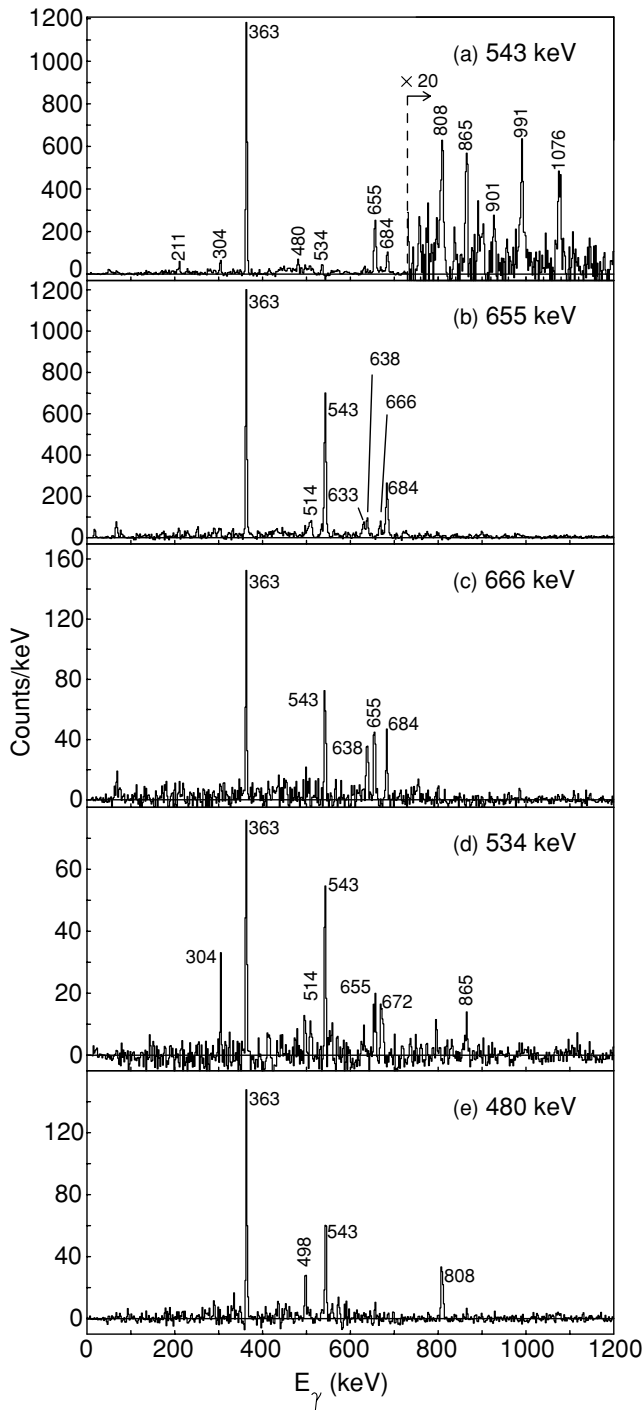


FIG. 4. γ -ray coincidence spectra correlated with the characteristic α decay of ^{167}Os . γ rays in coincidence with transitions of (a) 543 keV, (b) 655 keV, (c) 666 keV, (d) 534 keV, and (e) 480 keV are shown.

the protons were found to be inactive up to relatively high rotational frequency ($>0.5 \text{ MeV}/\hbar$).

The experimentally measured aligned angular momenta ($i_x = -de'/d\omega$) [27,28] for observed bands in ^{167}Os are shown in Fig. 9. A rotational reference, assuming a variable moment of inertia, has been subtracted from the data in accordance

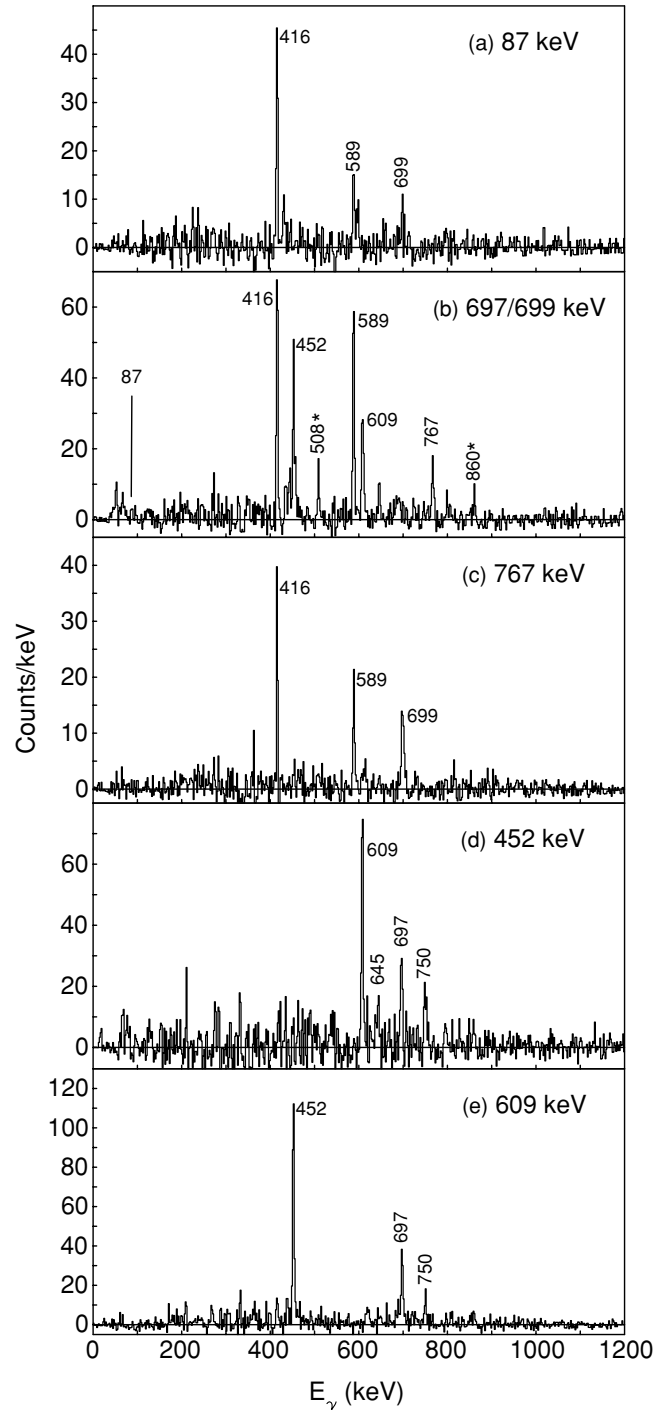


FIG. 5. γ -ray coincidence spectra correlated with the characteristic α decay of ^{167}Os . Gamma rays in coincidence with transitions of (a) 87 keV, (b) 697/699 keV, (c) 767 keV, (d) 452 keV, and (e) 609 keV are shown. For transitions marked with an asterisk, a lack of statistics has prevented them from being included in the ^{167}Os level scheme.

with the Harris formula [29], where $\mathfrak{S}_0 = 5\hbar^2 \text{ MeV}^{-1}$ and $\mathfrak{S}_1 = 111\hbar^4 \text{ MeV}^{-3}$. The reference has been chosen to give a near-constant alignment for the low-spin states of the yrast band.

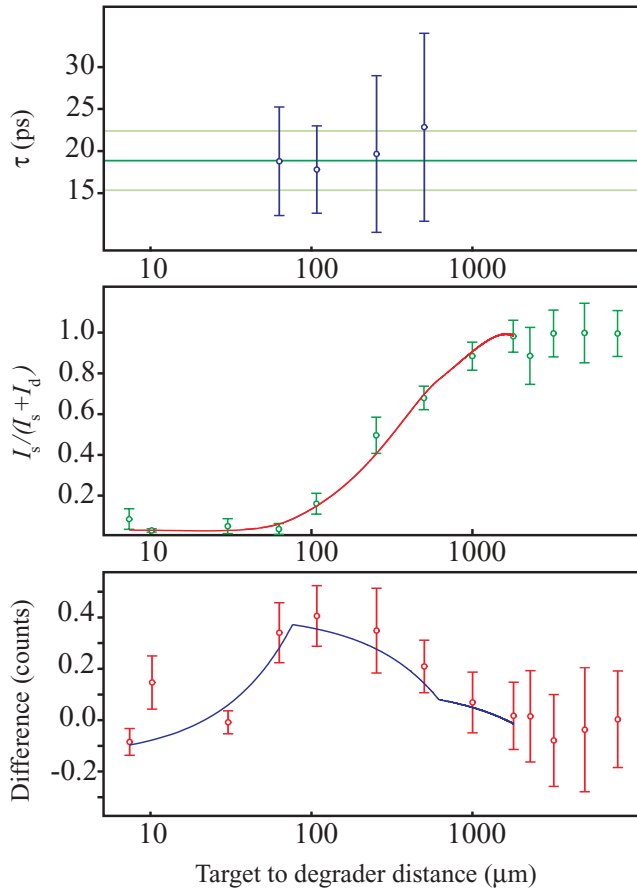


FIG. 6. (Color online) Lifetime determination, according to the principles of the DDCM, for the $17/2^+$ yrast state in ^{167}Os . Lifetime values calculated for different distances within the region of sensitivity are presented in the top panel. The decay curve, recorded with 10 Ge detectors at 134° is shown in the middle panel. The smooth line represents the fit to the decay curve. The bottom panel shows the difference of the quantities $I_s/(I_s + I_d)$ for the depopulating and direct feeding transitions. The line drawn through the experimental points is the derivative of the decay curve multiplied by the lifetime value.

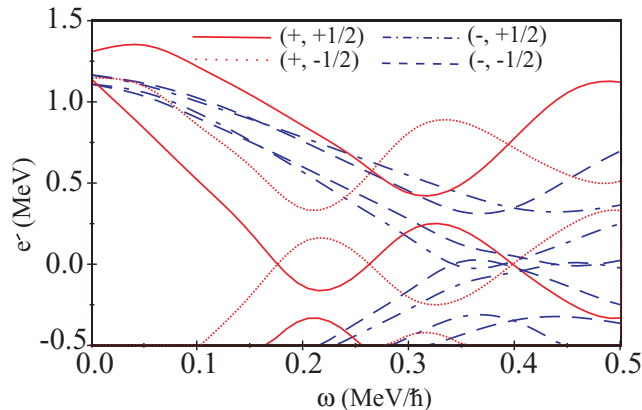


FIG. 7. (Color online) Cranked Woods-Saxon quasineutron Routhians for ^{167}Os with $\beta_2 = 0.16$, $\beta_4 = 0.004$, and $\gamma = 12^\circ$. The parity and signature (π, α) labeling of the orbitals is indicated.

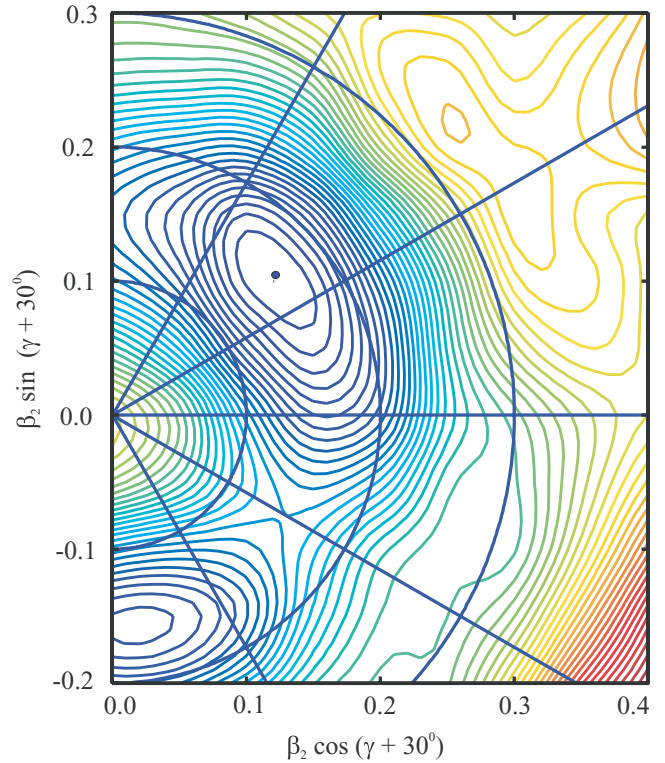


FIG. 8. (Color online) Total Routhian surface calculated for the $(\pi, \alpha) = (+, +1/2)$ configuration in ^{167}Os at $\hbar\omega = 0.12$ MeV. The absolute minimum is indicated by the dot. The energy difference between the contour lines is 100 keV.

A. Yrast band

Joss *et al.* [7] observed five states that were associated with yrast band of ^{167}Os with the highest state being tentatively assigned a spin and parity of $29/2^+$, which is confirmed in this work (see Table I). In this work the band has been extended up

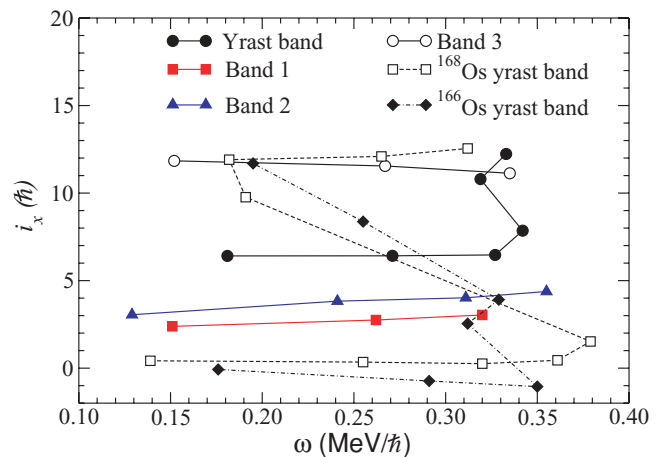


FIG. 9. (Color online) Experimental aligned angular momentum i_x as a function of rotational frequency ω for the bands in ^{167}Os observed in the present study. Also plotted are the yrast bands in ^{166}Os and ^{168}Os [7,30]. For Bands 1 and 2, values of $K = 7/2$ and $9/2$ have been used in accordance with the bandhead spins. In the case of the yrast band and Band 3 $K = 1/2$ has been used.

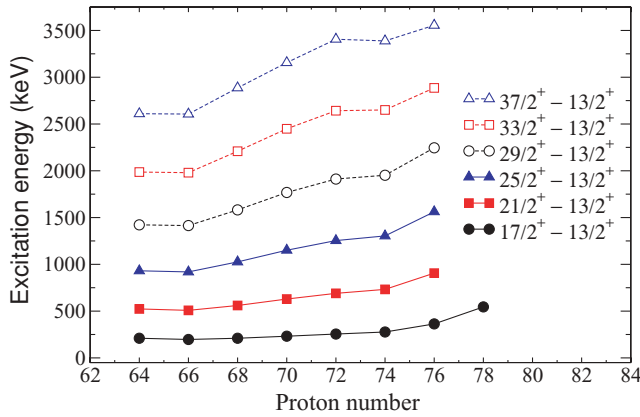


FIG. 10. (Color online) Comparison of yrast states of even- Z $N = 91$ isotones from Gd ($Z = 64$) to Pt ($Z = 78$). The data have been extracted from Refs. [31–37].

to $(37/2^+)$. With this extension it is interesting to examine the level energies of the odd- A $N = 91$ isotones as a function of proton number. This is shown in Fig. 10. The observed trend of increasing excitation energies with increasing proton number is a familiar one and is attributed to the filling of the $Z = 82$ shell and this trend continues for ^{167}Os even up to high spin.

The yrast band was associated [7] with the one quasineutron $i_{13/2}$ configuration in accordance with the observations in the heavier Os isotopes. Hence, the bandhead was tentatively assigned $I^\pi = 13/2^+$. This assumption has recently been confirmed by Scholey *et al.* According to the cranked Woods-Saxon calculations of the present work, this lowest-lying positive parity configuration ($\pi = +$, $\alpha = +1/2$) is calculated to carry an aligned angular momentum of $5.9\hbar$ at $\omega = 0.25$ MeV/ \hbar . This value is in reasonable agreement with the measured value for the yrast band of $6.5\hbar$ at $\omega = 0.25$ MeV/ \hbar . The first rotational alignment of a pair of $i_{13/2}$ quasineutrons, which is observed in the neighboring even-even nucleus ^{168}Os (see Fig. 9) is blocked in the yrast band of ^{167}Os . The first crossing is therefore expected to be caused by the second $i_{13/2}$ neutron alignment. Figure 7 shows that this crossing is predicted to be at $\omega \approx 0.32$ MeV/ \hbar . In this work a gain in aligned angular momentum is observed at $\omega \approx 0.33$ MeV/ \hbar , which is consistent with the start of this crossing.

The aligned angular momentum of the yrast band is plotted and compared with neighboring odd- A Os nuclei in Fig. 11(a). For ^{173}Os , the yrast band clearly displays a smooth upbend as rotational frequency is increased. However, in the case of ^{171}Os a clear backbend is observed. It was noted in Ref. [8] that this trend may indicate a weakening of the interaction strength [27,28] between the crossing configurations. Currently, no information is available to determine whether this behavior extends to ^{169}Os but the present study of ^{167}Os shows that the interaction strength of this crossing remains rather weak.

In Fig. 11(b) the observed aligned angular momentum of ^{167}Os is compared with other $N = 91$ isotones. In this case, the $Z = 70$ nucleus ^{161}Yb exhibits a clear upbend indicating a strong interaction between the one quasineutron band and the three quasineutron-band while a weakening of the interaction is evident from the back bending displayed

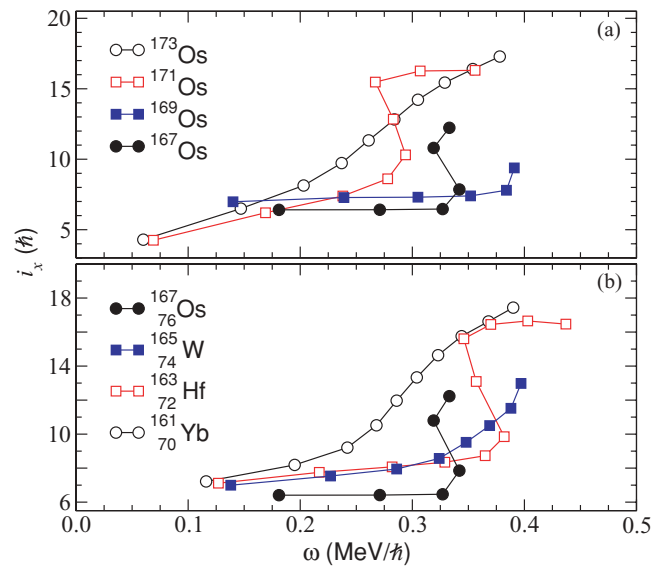


FIG. 11. (Color online) Experimental aligned angular momentum i_x as a function of rotational frequency ω of the ^{167}Os yrast band compared with (a) neighboring odd- A Os isotopes [8,19,21]; (b) the $N = 91$ isotones. In all cases, the alignments have been calculated using $K = 1/2$.

by ^{163}Hf . Insufficient data exist to make a firm conclusion regarding the behavior of ^{165}W . However, as mentioned above, the interaction strength of ^{167}Os is rather weak and does not appear to follow a systematic trend.

It is also interesting to note that, while the full crossing is not observed in ^{167}Os yrast band, the discontinuity in the aligned angular momentum for the highest spin state could indicate a crossing with a lower gain in aligned angular momentum than expected for an $(i_{13/2})^2$ crossing. This may be caused by a rather different underlying structure. Indeed, a lower alignment gain is also observed in ^{162}W , the lightest tungsten nucleus with data known to high-enough spin, where it is attributed to the rotational alignment of a pair of $h_{9/2}$ neutrons [38]. A similar discontinuity in the aligned angular momentum is also observed at the same rotational frequency in ^{166}Os , see Fig. 9, which may also be an indication of the effect of the $h_{9/2}$ orbital. Clearly further work to delineate the yrast band structures to higher spin in this nucleus and neighboring nuclei is required to gain a full understanding of all the alignment mechanisms.

B. Bands 1 and 2

The bands denoted Band 1 and Band 2 in Fig. 3 are reported here for the first time. Scholey *et al.* [11] have measured the spin and parity of the ground state and first excited state of ^{167}Os to be $7/2^-$ and $9/2^-$, respectively. It is speculated that these states result from the unpaired neutron occupying orbitals of the $f_{7/2}$ and $h_{9/2}$ single-particle states. In this work, Bands 1 and 2 constitute structures based on these states. Similar negative-parity structures have been reported by Bark *et al.* [19,21] in their study of the excited states of ^{171}Os and ^{173}Os . The ground states of these heavier isotopes were tentatively assigned $I^\pi = 5/2^-$ based on the assumption

that the unpaired neutron occupies an $\Omega = 5/2$ Nilsson orbital [19,21]. Figure 9 shows that Band 1 carries an average aligned angular momentum of $2.8 \hbar$ at $\omega \approx 0.25 \text{ MeV}/\hbar$ while Band 2 carries $3.8 \hbar$ at the same frequency. The cranking calculations predict that the lowest-energy negative-parity orbitals that are closest to the Fermi surface are based on the mixed $(f_{7/2}, h_{9/2})$ configurations; see Fig. 7. The calculations predict that the lowest energy negative-parity orbitals carry aligned angular momenta of $\approx 3.4\hbar$ and $2.6\hbar$, respectively, at $\omega = 0.25 \text{ MeV}/\hbar$, consistent with the values measured for Bands 1 and 2. It would be of importance to extend these structures to higher spin where the first $(i_{13/2})^2$ alignment would be expected to confirm these assignments.

C. Bands 3, 4, and 5

The aligned angular momentum of Band 3 is plotted in Fig. 9 and it can be seen that this band carries an alignment of $\approx 11.5\hbar$ at $\omega = 0.25 \text{ MeV}/\hbar$. The excitation energy of the band head is of the order of twice the neutron pairing gap ($2\Delta_v$) in ^{167}Os and in excess of $2\Delta_\pi$. Therefore, it is possible that this structure is the result of a three-quasiparticle configuration. Most likely is the three-quasineutron configuration $[f_{7/2}, h_{9/2} \otimes (i_{13/2})^2]$ because the CSM calculations suggest the protons remain inactive until very high rotational frequencies. However, the possibility that Band 3 involves a pair of quasiprotons cannot be ruled out based on the experimental data alone.

As very few states have been associated with the decay of Bands 4 and 5, it is not meaningful to discuss in any detail the possible microscopic structure of these bands. However, as is the case for Band 3 above, the excitation energy and spin of the bandheads suggests they may also be three-quasineutron excitations.

D. Quadrupole deformation in ^{167}Os

The measured lifetime of the $17/2^+$ state corresponds to a reduced transition probability $B(E2)$ of 120(20) W.u. This high $B(E2)$ value confirms the collective nature of the $17/2^+ \rightarrow 13/2^+$ transition, which is expected in the vicinity of the neutron midshell.

An absolute value of the transition quadrupole moment Q_t can be extracted from the measured $B(E2)$ value within the rotational model [39]. Assuming $K = 1/2$ for the yrast band of ^{167}Os , a value of $|Q_t| = 4.4(4) \text{ eb}$ is deduced. Furthermore, by using the deformation parameters ($\beta_2 = 0.16$, $\beta_4 = 0.004$, $\gamma = 12^\circ$) obtained from the TRS calculations discussed above, a transition quadrupole moment can be calculated from [10]

$$Q_t = \frac{6ZeA^{2/3}}{(15\pi)^{1/2}} r_0^2 \beta_2 \left[1 + \frac{2}{7} \left(\frac{5}{\pi} \right)^{1/2} \beta_2 \right] \cos(30^\circ + \gamma),$$

where $r_0 = 1.2 \text{ fm}$. The TRS calculations predict $Q_t = 3.6 \text{ eb}$. A comparison with the experimentally deduced value shows that the TRS calculations reproduce the deformed character of the $(\pi, \alpha) = (+, +1/2)$ configuration in ^{167}Os . However, the experimental $|Q_t|$ value is slightly larger than that suggested by theory.

Prior to the present study, the lightest Os nucleus in which the extent of deformation was reported was $^{172}\text{Os}_{96}$ [10]. In this previous work, the lifetimes of the yrast states up to $I = 20\hbar$ were measured in addition to five states comprising a negative-parity band. Virtanen *et al.* [10] reported a transition quadrupole moment of $Q_t = 5.7(3) \text{ eb}$ for the $I^\pi = 2^+$ state of ^{172}Os , which suggests that this nucleus is significantly more deformed than ^{167}Os . The reduction in quadrupole deformation is not unexpected with the reduction in the number of valence neutrons as the spherical shell closure at $N = 82$ is approached.

E. Summary

The level scheme of ^{167}Os has been extended using the recoil-decay tagging technique and γ - γ and angular-intensity measurements. Band structures have been established based on the ground state and lowest excited states, including extending the band based on the $\nu i_{13/2}$ isomeric state to higher spin. Experimental observations have been compared with theoretical calculations based on the cranked shell model. Evidence for the $\nu i_{13/2}$ neutron alignment is established in the yrast band. Furthermore, the lifetime of the $17/2^+$ state of the yrast band has been measured, which is consistent with quadrupole deformed character. This study represents the most neutron-deficient Os isotope in which the deformation has been measured.

ACKNOWLEDGMENTS

Financial support for this work has been provided by the UK Science and Technology Facilities Council (STFC) and by the EU 6th Framework Programme, "Integrating Infrastructure Initiative—Transnational Access," contract number 506065 (EURONS), and by the Academy of Finland under the Finnish Centre of Excellence Programme 2006–2011 (Nuclear and Accelerator Based Physics Programme at JYFL). P.T.G. and C.S. acknowledge the support of the Academy of Finland. The authors express their gratitude to the staff of the Accelerator Laboratory at the University of Jyväskylä for their excellent technical support. The authors also thank Paul Morrall of Daresbury Laboratory for preparation of the Mo targets, which made this work possible and Neil Rowley of IN2P3 (France) for stimulating discussions regarding the interpretation of experimental observations.

[1] K.-H. Schmidt, R. S. Simon, J.-G. Keller, F. P. Hessberger, G. Münzenberg, B. Quint, H.-G. Clerc, W. Schwab, U. Gollerthan, and C.-C. Sahn, Phys. Lett. **B168**, 39 (1986).

[2] R. S. Simon, K. H. Schmidt, F. P. Heßberger, S. Hlavac, M. Honusek, G. Münzenberg, H. G. Clerc, U. Gollerthan, and W. Schwab, Z. Phys. A **325**, 197 (1986).

- [3] E. S. Paul, P. J. Woods, T. Davinson, R. D. Page, P. J. Sellin, C. W. Beusang, R. M. Clark, R. A. Cunningham, S. A. Forbes, D. B. Fossan *et al.*, *Phys. Rev. C* **51**, 78 (1995).
- [4] D. T. Joss, K. Lagergren, D. E. Appelbe, C. J. Barton, J. Simpson, B. Cederwall, B. Hadinia, R. Wyss, S. Eeckhauht, T. Grahn *et al.*, *Phys. Rev. C* **70**, 017302 (2004).
- [5] S. L. King, R. D. Page, J. Simpson, A. Keenan, N. Amzal, A. J. Chewter, J. F. Cocks, D. M. Cullen, O. Dorvaux, P. T. Greenlees *et al.*, *Phys. Rev. C* **62**, 067301 (2000).
- [6] D. E. Appelbe, J. Simpson, M. Muikku, H. J. Boardman, A. Melarangi, R. D. Page, P. T. Greenlees, P. M. Jones, R. Julin, S. Juutinen *et al.*, *Phys. Rev. C* **66**, 014309 (2002).
- [7] D. T. Joss, S. L. King, R. D. Page, J. Simpson, A. Keenan, N. Amzal, T. Bäck, M. A. Bentley, B. Cederwall, J. F. C. Cocks *et al.*, *Nucl. Phys.* **A689**, 631 (2001).
- [8] D. T. Joss, J. Simpson, R. D. Page, S. L. King, N. Amzal, D. E. Appelbe, T. Bäck, M. A. Bentley, B. Cederwall, J. F. Cocks *et al.*, *Phys. Rev. C* **66**, 054311 (2002).
- [9] P. M. Davidson, G. D. Dracoulis, T. Kibédi, A. P. Byrne, S. S. Anderssen, A. M. Baxter, B. Fabricius, G. J. Lane, and A. E. Stuchbery, *Nucl. Phys.* **A568**, 90 (1994).
- [10] A. Virtanen, N. R. Johnson, F. K. McGowan, I. Y. Lee, C. Baktash, M. A. Riley, J. C. Wells, and J. Dudek, *Nucl. Phys.* **A591**, 145 (1995).
- [11] C. Scholey *et al.* (to be submitted to *Phys. Rev. C*).
- [12] C. W. Beusang and J. Simpson, *J. Phys. G: Nucl. Part. Phys.* **22**, 527 (1996).
- [13] M. Leino, J. Aysto, T. Enqvist, P. Heikkinen, A. Jokinen, M. Nurmi, A. Ostrowski, W. H. Trzaska, J. Uusitalo, K. Eskola *et al.*, *Nucl. Instrum. Methods Phys. Res., B* **99**, 653 (1995).
- [14] R. D. Page, A. N. Andreyev, D. E. Appelbe, P. A. Butler, S. J. Freeman, P. T. Greenlees, R.-D. Herzberg, D. G. Jenkins, G. D. Jones, P. Jones *et al.*, *Nucl. Instrum. Methods Phys. Res., B* **204**, 634 (2003).
- [15] R. D. Page, P. J. Woods, R. A. Cunningham, T. Davinson, N. J. Davis, A. N. James, K. Livingston, P. J. Sellin, and A. C. Shotton, *Phys. Rev. C* **53**, 660 (1996).
- [16] R. A. Bark, *Nucl. Instrum. Methods Phys. Res., A* **595**, 637 (2008).
- [17] D. C. Radford, *Nucl. Instrum. Methods Phys. Res., A* **361**, 297 (1995).
- [18] A. Dewald, S. Harissopulos, and P. von Brentano, *Z. Phys. A* **334**, 163 (1989).
- [19] R. A. Bark, G. D. Dracoulis, and A. E. Stuchbery, *Nucl. Phys.* **A514**, 503 (1990).
- [20] C. A. Kalfas, S. Kossionides, C. T. Papadopoulos, R. Vlastou, L. Hildingsson, W. K. Lamra, T. Lindblad, C. G. Lindén, R. Wyss, J. Gizon *et al.*, *Nucl. Phys.* **A526**, 205 (1991).
- [21] R. A. Bark, S. Törmänen, T. Bäck, B. Cederwall, S. W. Ødegård, J. F. C. Cocks, K. Helariutta, P. Jones, R. Julin, S. Juutinen *et al.*, *Nucl. Phys.* **A646**, 399 (1999).
- [22] T. Grahn, A. Dewald, O. Möller, R. Julin, C. W. Beusang, S. Christen, I. G. Darby, S. Eeckhauht, P. T. Greenlees, A. Görgen *et al.*, *Nucl. Phys.* **A801**, 83 (2008).
- [23] S. Cwiok, J. Dudek, W. Nazarewicz, W. Skalski, and T. Werner, *Comput. Phys. Commun.* **46**, 379 (1987).
- [24] W. Satula, R. Wyss, and P. Magierski, *Nucl. Phys.* **A578**, 45 (1994).
- [25] W. Satula and R. Wyss, *Phys. Scr., T* **56**, 159 (1995).
- [26] W. Nazarewicz, J. Dudek, R. Bengtsson, T. Bengtsson, and I. Ragnarsson, *Nucl. Phys.* **A435**, 397 (1985).
- [27] R. Bengtsson and S. Frauendorf, *Nucl. Phys.* **A314**, 27 (1979).
- [28] R. Bengtsson and S. Frauendorf, *Nucl. Phys.* **A327**, 139 (1979).
- [29] S. M. Harris, *Phys. Rev.* **138**, B509 (1965).
- [30] D. E. Appelbe, J. Simpson, M. Muikku, H. J. Boardman, A. Melarangi, R. D. Page, P. T. Greenlees, P. M. Jones, R. Julin, S. Juutinen *et al.*, *Phys. Rev. C* **66**, 014309 (2002).
- [31] C. W. Reich, *Nucl. Data Sheets* **104**, 1 (2005).
- [32] T. Hayakawa, Y. Toh, M. Oshima, M. Matsuda, Y. Hatsukawa, J. Katakura, H. Iimura, T. Shizuma, S. Mitarai, M. Sugawara *et al.*, *Eur. Phys. J. A* **15**, 299 (2002).
- [33] R. G. Helmer, *Nucl. Data Sheets* **99**, 483 (2003).
- [34] C. W. Reich and R. G. Helmer, *Nucl. Data Sheets* **90**, 645 (2000).
- [35] K. P. Blume, H. Hübel, M. Murzel, J. Recht, K. Theine, H. Kluge, A. Kuhnert, K. H. Maier, A. Maj, M. Guttormsen *et al.*, *Nucl. Phys.* **A464**, 445 (1987).
- [36] J. Simpson, F. Hanna, M. A. Riley, A. Alderson, M. A. Bentley, A. M. Bruce, D. M. Cullen, P. Fallon, and L. Walker, *J. Phys. G: Nucl. Part. Phys.* **18**, 1207 (1992).
- [37] D. T. Joss, J. Simpson, D. E. Appelbe, C. J. Barton, D. D. Warner, K. Lagergren, B. Cederwall, B. Hadinia, S. Eeckhauht, T. Grahn *et al.*, *Phys. Rev. C* **74**, 014302 (2006).
- [38] G. Dracoulis, B. Fabricius, P. M. Davidson, A. O. Macchiavelli, J. Oliviera, J. Burde, F. Stephens, and M. A. Deleplanque, in *Proceedings of the International Conference on Nuclear Structure at High Angular Momentum, Ottawa, Ontario, 1992*, edited by D. Ward and J. C. Waddington (AECL Research Report No. AECL-10613), Vol. II, p. 94.
- [39] A. Bohr and B. Mottelsson, *Nuclear Structure* (Benjamin, New York, 1975), Vol. 2, p. 45.